Journal of Mechatronics, Electrical Power, and Vehicular Technology

LSTM-based forecasting on electric vehicles battery swapping demand: Addressing infrastructure challenge in Indonesia

Muhammad Zakiyullah Romdlony [a], Rashad Abul Khayr [a, *], Aam Muharam [b],
Eka Rakhman Priandana [c], Sudarmono Sasmono [a], Muhammad Ridho Rosa [a, e],
Irwan Purnama [a, d], Amin [b], Ridlho Khoirul Fachri [a]

[a] School of Electrical Engineering, Telkom University
Jalan Telekomunikasi Terusan Buah Batu, Bandung, 40257, Indonesia

[b] Research Center for Transportation Technology, National Research and Innovation Agency (BRIN)
Kawasan Sains dan Teknologi (KST) Habibie, Jalan Raya Puspiptek – Serpong, Tangerang Selatan, 15310, Indonesia

[c] Research Center for Energy Conversion and Conservation, National Research and Innovation Agency (BRIN)
Kawasan Sains dan Teknologi (KST) Habibie, Jalan Raya Puspiptek – Serpong, Tangerang Selatan, 15310, Indonesia

[d] Research Center for Smart Mechatronics, National Research and Innovation Agency (BRIN)
Kawasan Sains dan Teknologi (KST) Samadikun, Jalan Cisitu – Sangkuriang, Bandung, 40135, Indonesia

[e] Faculty of Science and Engineering, University of Groningen
Nijenborgh 4, Groningen, 9747 AG, The Netherlands

Abstract

This article aims to design a model for forecasting the number of vehicles arriving at the battery swap station (BSS). In our case, we study the relevance of the proposed approach given the rapid increase in electric vehicle users in Indonesia. Due to the vehicle electrification program from the government of Indonesia and the lack of supporting infrastructure, forecasting battery swap demands is very important for charging schedules. Forecasting the number of vehicles is done using machine learning with the long short-term memory (LSTM) method. The method is used to predict sequential data because of its ability to review previous data in addition to the current input. The result of the forecasting using the LSTM method yields a prediction score using the root-mean-square error (RMSE) of 2.3079×10^{-6}. The forecasted data can be combined with the battery charging model to acquire predicted hourly battery availability that can be processed further for optimization and scheduling.

I. Introduction

Machines that require combustion as the primary energy generator, such as those in factories and motor vehicles, produce hazardous gases. These gases play an active role in the increase in Earth's temperature. This increase in temperature is caused by the effect of gases that can reflect the sun's heat that is supposed to come out of the Earth's atmosphere back to the Earth's surface. Rising global temperatures can lead to natural disasters. Therefore, the United Nations (UN) signed the agreement to reduce these hazardous gas emissions called the Paris Agreement on 12 December 2015 [1]. This agreement aims to address climate change by reducing greenhouse gas emissions that can reflect solar heat. To support this cooperation, greenhouse gas sources such as motor vehicles must be reduced. However, motor vehicles are widely used in everyday life and are difficult to reduce. Therefore, it is necessary to replace motor vehicles that have lower or no emissions.

Indonesia has implemented regulations to reduce emissions from motor vehicles by instituting CO_2 reduction in the transportation sector, i.e., the use of electric vehicles. With the release of Presidential Regulation 55/2019 on battery-powered electric

vehicles, the popularity of electric vehicles began to increase once more. In addition, the local government has enacted a number of subsidiary policies to expedite the creation of electric vehicles. As a consequence of this regulation, there is a surge in the number of electric vehicles, particularly electric motorcycles. Some motorcycles brands have been manufactured in the country, resulting in a rapid increase in the number of electric vehicles by 2020 [2].

These electric vehicles require an energy source, but their small shape makes electric vehicles only use batteries as their energy source. The use of this battery will cause problems with charging the battery itself. The battery requires high power. This will increase considering the increasing consumption of electric vehicles. This power use should be scheduled so that the user does not wait long and there is no surge in power use. Scheduling from battery charging can be charging at a time that not many users use [3][4][5], combined with renewable energy [6][7][8], or trying to increase profits [9][10]. The scheduling method mentioned above requires an accurate prediction of battery availability to be implemented correctly. To achieve acceptable accuracy, battery availability can be predicted using battery demand and battery charging methods. This study aims to develop an accurate prediction of battery availability by using forecasted battery demand and battery charge time using commonly used charging methods.

II. Materials and Methods

Battery availability for a battery swap station (BSS), as mentioned in the introduction, can be predicted using vehicle arrivals and battery charging times. Battery charging can be achieved by using the appropriate battery charging model. There are many charging models that can be used by electric vehicle batteries. But as mentioned later, only one model is commonly used by electric vehicle batteries due to ease of implementation.

Battery demand data for battery availability can be acquired by using forecasting. Data from the past can be processed using a neural network (NN), and the number of vehicles that use the BSS for a given time frame can be acquired. Data acquired from a NN can be used to represent battery demands, assuming that one vehicle only swaps for a single battery.

In the following subsections, we will elaborate more about the battery charging model, forecasting model, and parameter used for simulation.

A. Battery charging model

Lithium batteries are widely used for electric vehicles due to their high energy density and open-circuit voltage. Because of its high energy density, this type of battery is prone to exploding at high temperatures. To anticipate such incidents, especially when charging, lithium batteries require a specialized charging method. There are many

charging methods that can be used to charge lithium batteries, with varying efficiency and complexity.

The charging method constant current (CC), constant voltage (CV), and constant power (CP) are the least complex charging methods but also the least efficient, with the highest possibility of damaging the battery during charging [11]. Another method is electrochemical model-based charging, which produces the highest efficiency but also has a high complexity, making implementation of this method difficult [12]. The last method to consider is constant current-constant voltage (CCCV), which has average efficiency and average complexity compared to other charging methods. But with its low complexity, the CCCV method has become the most commonly used due to its ease of implementation while still maintaining an acceptable level of efficiency.

The CCCV method begins with a CC until a predetermined voltage is reached. Once the voltage reaches this threshold, the charging voltage becomes constant while the charging current decreases exponentially [9][13]. Increased internal resistance causes a decrease in current during CV operation. This resistance will increase as the battery's temperature and state of charge (SoC) increase during charging [14]. When charging in the CC stage, only the charging voltage is affected by the battery's internal resistance. After the charging change stage, the current will decrease exponentially as the internal resistance increases. The charging current for CC-CV methods for both stages is depicted in Figure 1.

This battery charging method will be required in the formation of the schedule for the battery swap station (BSS). With the correct charging model, the scheduling of the BSS will be more efficient. It also requires calculating the SoC of the battery shown in equation (1).

$$K = K_0 + \int \frac{I_b}{C_b} dt \tag{1}$$

The SoC of the battery (K) will depend on the SoC before charging (K_0), charging current (I_b), and battery capacity that can be used. (C_b). It can be seen from the equation that the SoC of a battery will depend on the health of the battery itself. In addition, the charging current will determine sooner or later when the battery is charged [15].

B. Forecasting model

Sequential data can be predicted using artificial intelligence. This intelligence can be created with various machine learning methods, such as artificial neural networks (ANNs). ANN is a machine learning method inspired by early models of sensory processing in the brain. This can be simulated using a network of neuron models on a computer. The network can break a feature from the input so that the computer can identify the input from the feature it has learned. Because this machine can learn, ANN is widely used in classification problems [16]. These ANNs will develop into recurrent neural networks (RNNs) to process sequential data.
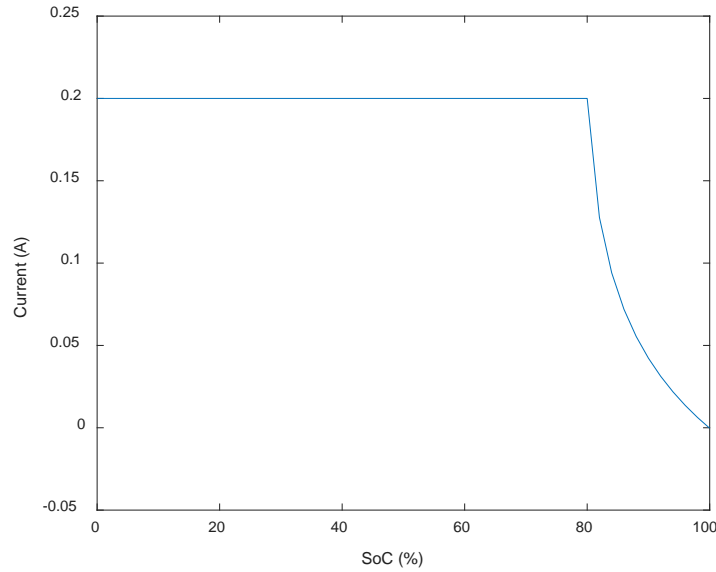
Figure 1. Battery charging current with CC-CV charging method

RNNs have an architecture where there is a layer (hidden layer or output layer) that becomes the input of the input layer. The architecture allows this method to detect relationships sequentially. This method developed rapidly with the emergence of long short-term memory (LSTM) and gated recurrent unit (GRU), which made it possible to remember distant past circumstances [17]. The ability to make predictions with past data makes scheduling methods like the day-ahead method possible [6].

GRU is a type of RNN that aims to resolve problems in the long term by using reset and update gates. Both gates are used to measure the correlation between the previous state and the next forecasting step. GRU can be trained using a smaller dataset than LSTM. By using a smaller dataset, GRU can be trained faster due to the two gates of GRU [18][19].

LSTM is a development of RNN that can remember information for a longer period of time than RNN. This is due to the addition of memory blocks to an RNN cell, where RNN cells themselves are a group of RNN networks. This additional memory block makes LSTM more accurate than GRU with a larger dataset and a longer training time. As accuracy is valued more than time, forecasting using LSTM was considered the main model for this article. The additional memory blocks are arranged in three-gates: Input Gate ($i_{(t)}$), Output gate ($o_{(t)}$), and Forget Gate ($f_{(t)}$) [20][21][22]. This arrangement for the LSTM cell can be seen in Figure 2.

Based on Figure 2, LSTM cells can be represented in mathematical equations as equation (2) to equation (7).

$$f_{(t)} = \sigma\big(W_{fx}x_{(t)} + W_{fh}h_{(t-1)} + b_f\big) \tag{2}$$

$$i_{(t)} = \sigma\big(W_{ix}x_{(t)} + W_{ih}h_{(t-1)} + b_i\big) \tag{3}$$

$$o_{(t)} = \sigma\big(W_{ox}x_{(t)} + W_{oh}h_{(t-1)} + b_o\big) \tag{4}$$

$$\tilde{p}_{(t)} = \tanh\big(W_{px}x_{(t)} + W_{ph}h_{(t-1)} + b_p\big) \tag{5}$$

$$p_{(t)} = f_{(t)} \cdot p_{(t-1)} + i_{(t)} \cdot \tilde{p}_{(t)} \tag{6}$$

$$h_{(t)} = o_{(t)} \cdot \tanh\big(p_{(t)}\big) \tag{7}$$

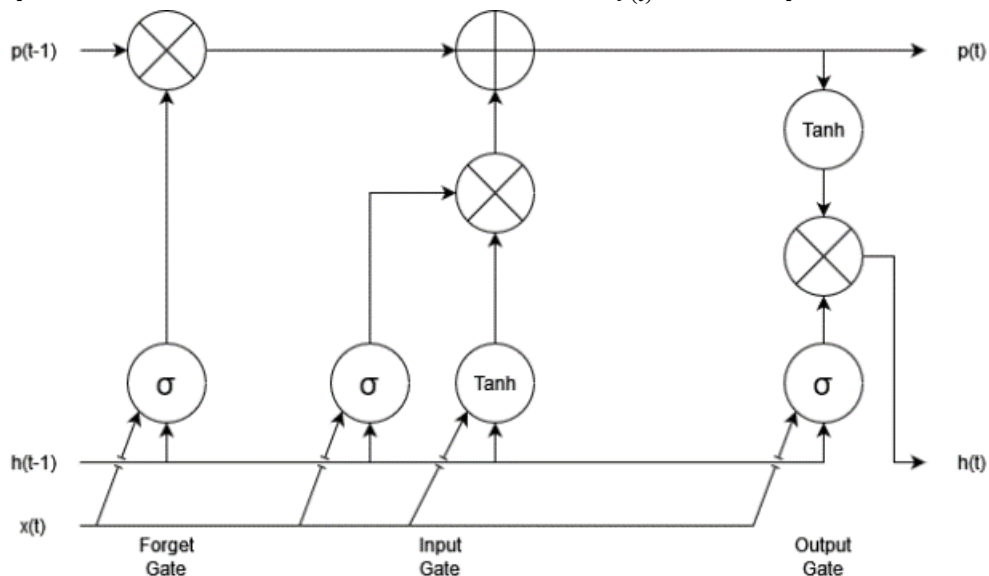where $p_{(t)}$ shows the previous cell memory and $h_{(t)}$

Figure 2. LSTM cell structure

Table 1.
Simulation parameter

Parameter	Value
Battery voltage	75 V
Charge current	5 A and 2 A
Battery capacity	20 Ah
Battery charging slot	12
Maximum available battery	9

is the output of the cell. b_f, b_i, b_o, and b_p are bias of each gate and predicted memory. W_{fx}, W_{ix}, W_{ox}, and W_{px} are the weights for input, while W_{fh}, W_{ih}, W_{oh}, and W_{ph} themselves are those for cell output that all have their own values depending on the gate and predicted memory. The values of the weight and bias will be replaced by the machine so that the predictive value is close to the training data value. Sigmoid (σ) and hyperbolic (tanh) functions are defined as equation (8) and equation (9).

$$\sigma(x) = \frac{1}{1+e^{-x}} \tag{8}$$

$$\tanh(x) = \frac{e^x - e^{-x}}{e^x + e^{-x}} \tag{9}$$

C. Simulation parameter

Both models required a predefined parameter to achieve an accurate prediction of battery availability. For prediction simulation, battery heterogeneity was not considered, as BSS for this simulation can only serve one type of battery. A battery that is commonly used for two-wheel electric vehicles in Indonesia was considered for this simulation. For lithium-ion (Li-ion) batteries, the battery parameter is shown in Table 1 alongside the BSS parameter and the available commercial charger for charge current.

The battery specified in Table 1 during extensive use can be used for around two hours. Considering extensive use and BSS peak hours, a dataset was generated with tendencies for single days, as shown in Figure 3. Peak hour was considered to happen between 15 o'clock and 19 o'clock, when students and workers were going home. Other possible peaks,

like before leaving home and around lunch, were also considered for the dataset.

The dataset used for this simulation is randomly generated. Both models required a predefined parameter to achieve an accurate prediction of battery availability. For prediction simulation, battery heterogeneity was not considered, as BSS for this simulation can only serve one type of battery. A battery that is commonly used for two-wheel electric vehicles in Indonesia was considered for this simulation. For Li-ion batteries, the battery parameter is shown in Table 1 alongside the BSS parameter.

III. Results and Discussions

The battery charging model and the forecasting model described earlier were tested using the parameters mentioned above. The battery charging model was tested using the parameters shown in Table 1. The effects of charge current and SoC threshold were also tested to find their connection to battery charging time. The forecasting model was trained using the generated dataset mentioned above and scored using the root-mean-square error (RMSE) to quantify forecasting model quality. After testing, these two models were combined to create a prediction for battery availability.

A. Battery charging

The effect of the current on battery charging can be tested with equation (1). With the same initial health and SoC, battery charging with a current of 0.25 C and 0.1 C was tested, with C being the
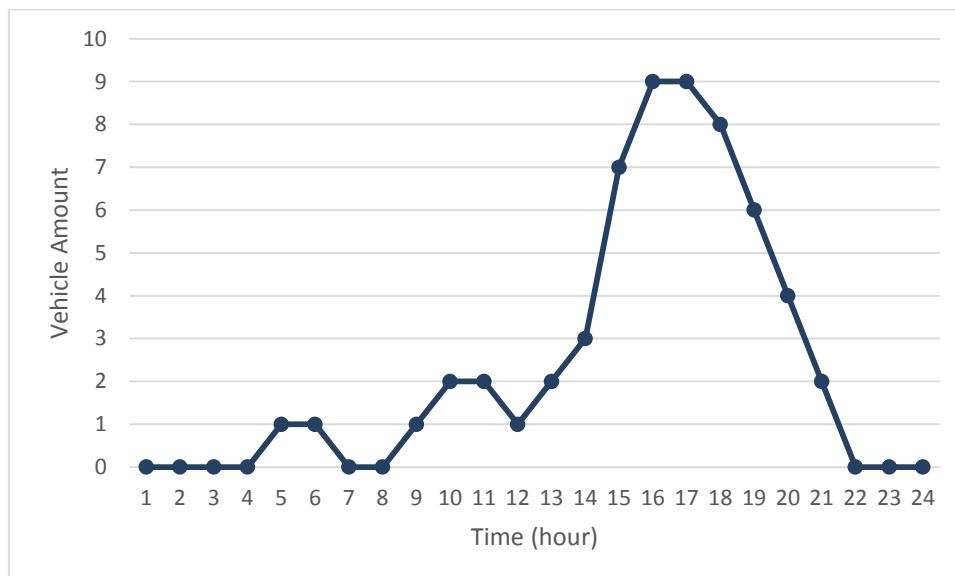

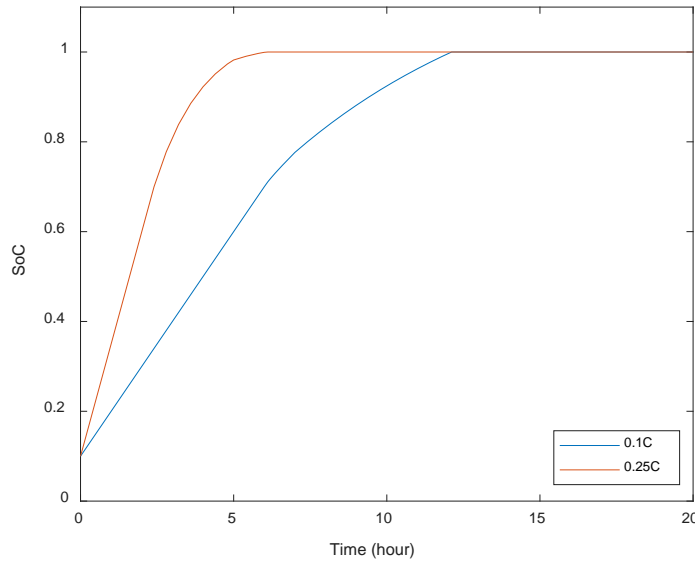Figure 3. Hourly vehicle amounts for one day

Figure 4. Comparison of different charge current effects for battery SoC with the CCCV charging method
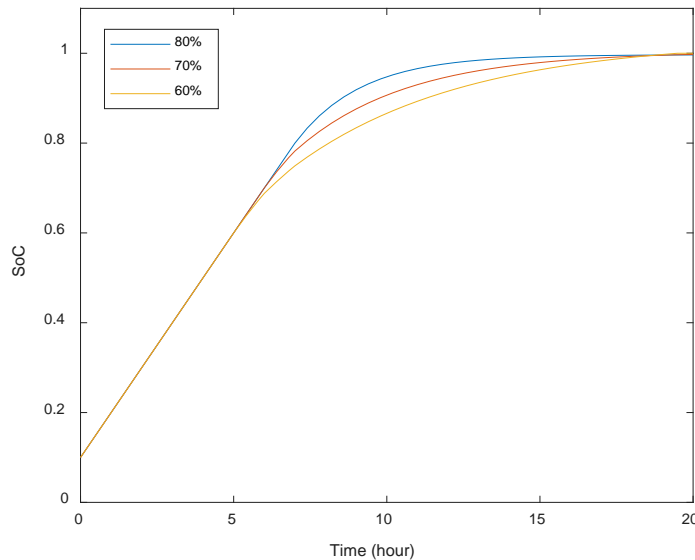

Figure 5. Comparison of different voltage cutoff effects for battery SoC with the CCCV charging method

battery's maximum capacity. The results of this test are shown in Figure 4.

The charging results show the effect of current on battery charging time. It appears that charging using 0.25 C reaches 80 % SoC in three hours, while charging with 0.1 C achieves the same in seven hours. This shows the advantages of high-current charging, but high-current charging will cause heat and reduce the health of the battery.

The test uses a battery charger with the same CCCV voltage limit. Because the voltage limit is a constant that has been set on the previous battery charger, these numbers can be modified and tested for their effects. For this test, the limits of 80 %, 70 %, and 60 % SoC were tested with a charging current of 0.1 C. The result of this test is shown in Figure 5.

Figure 5 shows charging differences with previously specified voltage limits, indicating changes in battery charging time. The difference between 80 % and 70 % shows that it takes 6

minutes to reach the 80 % SoC. The difference between the limit of 70 % and 60 % indicates one hour to reach an 80 % SoC. These tests showed that increased voltage limits would result in the battery reaching a SoC of 80 % faster without considering battery health.

B. Vehicle forecasting

LSTM has the ability to predict sequential data from previous time series. In this paper, we use randomly generated historical data on vehicle arrivals at BSSs. In addition to its architecture that takes input from other layers, LSTM is a predictive method that is suitable for predicting the number of vehicles coming every hour. It is known that the vehicle is coming, so that the battery replacement station can prepare the batteries to be removed. Figure 6 shows the prediction results of vehicle amounts using LSTM for ten days or 240 hours to show the effect of previous days.
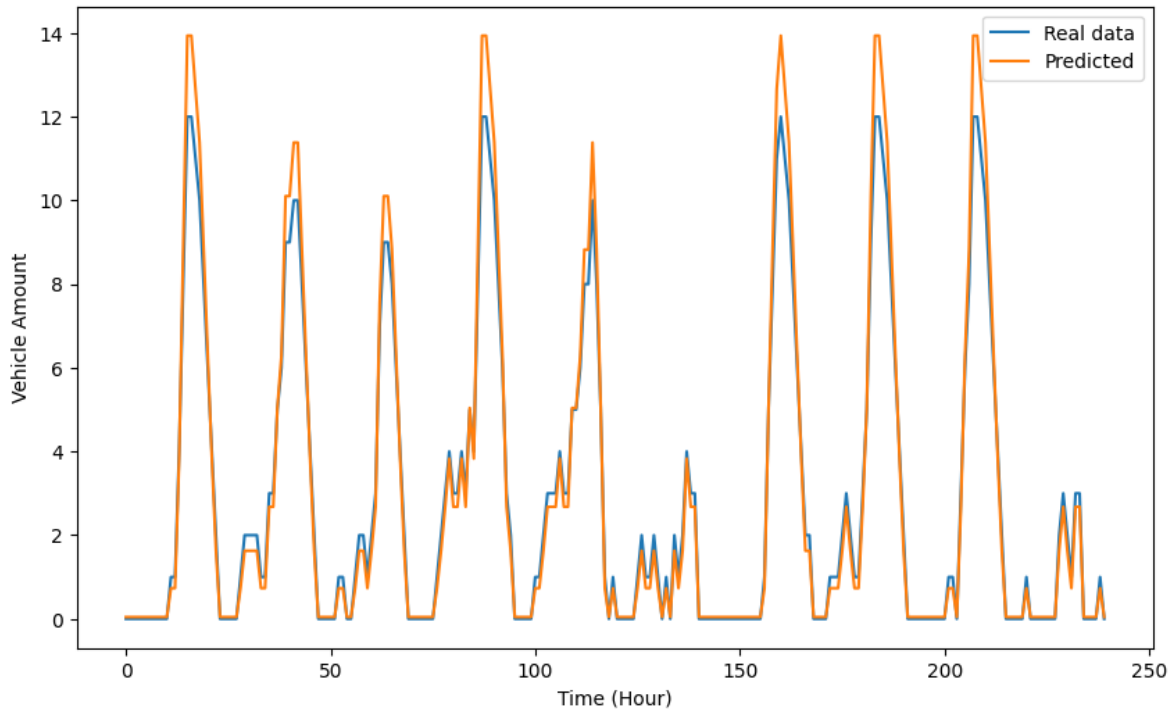
Figure 6. Comparison of real and predicted hourly vehicle amounts

The result of the prediction using LSTM results in a RMSE score of 2.3079×10^{-6}. The score is small enough for RMSE to be used for scheduling battery replacement stations.

C. Battery availability

Battery charging models and vehicle forecasting were combined to predict hourly battery availability. The prediction was made using hourly vehicle amounts, as shown in Figure 3, and parameters, as shown in Table 1, with the SoC threshold at 80 %. For this simulation, the battery is considered swappable when the SoC reaches 80 % with a uniform depth of discharge (DoD) of 100 % for every battery swap. The result of battery availability prediction is shown in Figure 7. Charge currents during CC are 2 A and 5 A.

BSS was having difficulty meeting battery swap demand at peak hours. Battery availability was a constant zero from hours 15 to 20 for 5 A charging current and from hours 14 to 21 for 2 A. The unmet battery swap demand during zero battery availability for 5 A and 2 A charging currents is shown in Figure 8.

Figure 8 shows BSS's difficulty meeting battery demand during peak hours. This unmet demand comes from high demand that can be seen in hours 16 to 17, where demand reaches nine batteries, or equal to the maximum battery available. Another factor is the slow charge time that can be seen in BSS with a 2 A charge current, which is unable to restore its battery availability to the maximum at the end of the day.
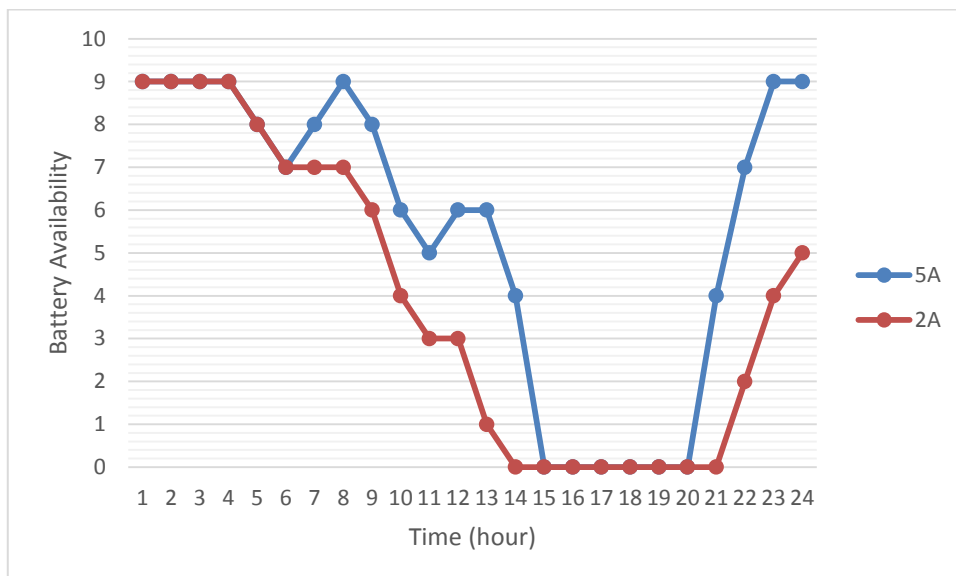

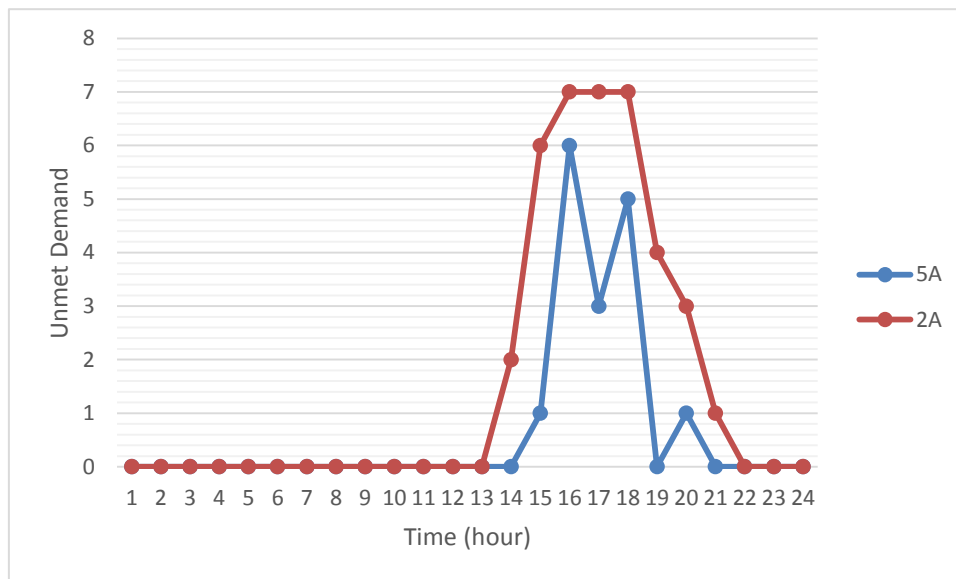Figure 7. Comparison of BSS battery availability for charge current 5 A and 2 A

Figure 8. Comparison of BSS unmet demands for charge current 5 A and 2 A

IV. Conclusion

This study aims to develop an accurate prediction of battery availability by using forecasted battery demand and battery charge time using commonly used charging methods. Simulation shows that the combination of battery charging methods using CCCV and forecasting using the LSTM model can be used to predict battery availability. The simulation also shows BSS's difficulty meeting battery demand during peak hours. That is because battery swap demands are equal to or greater than the maximum battery availability. Another reason is that it takes three hours to seven hours for the battery to charge to SoC 80%, depending on the charge current. Future research efforts will focus on optimizing adaptive charging, which can change its charging current to either meet battery demand or conserve battery health.

Acknowledgements

Declarations

Author contribution

M.Z. Romdlony, R.A. Khayr, A. Muharam, E.R. Priandana, S. Sasmono, M.R. Rosa, I. Purnama, Amin, R.K. Fachri contributed equally as the main contributor to this paper. All authors read and approved the final paper.

Funding statement

Competing interest

The authors declare that they have no known competing financial interests or personal relationships that could have appeared to influence the work reported in this paper.

Additional information

Reprints and permission: information is available at https://mev.lipi.go.id/.

Publisher's Note: National Research and Innovation Agency (BRIN) remains neutral with regard to jurisdictional claims in published maps and institutional affiliations.

References

[1] United Nations Climate Change. The Paris Agreement. [Accessed: 8-June-2023].

[2] The Central Government. Presidential Regulations on Accelerating the Battery-Based Electric Vehicle Program for Road Transport. [Accessed: 7-June-2023].

[3] Y. Li *et al.*, "Optimal scheduling of isolated microgrid with an electric vehicle battery swapping station in multi-stakeholder scenarios: A bi-level programming approach via real-time pricing," *Appl. Energy*, vol. 232, pp. 54–68, Dec., 2018.

[4] M. Sufyan, N. A. Rahim, M. A. Muhammad, C. K. Tan, S. R. S. Raihan, and A. H. A. Bakar, "Charge coordination and battery lifecycle analysis of electric vehicles with V2G implementation," *Electric Power Systems Research*, vol. 184, p. 106307, Jul., 2020.

[5] J. G. -Guarin, W. Infante, J. Ma, D. Alvarez, and S. Rivera, "Optimal scheduling of smart microgrids considering electric vehicle battery swapping stations," *International Journal of Electrical and Computer Engineering (IJECE)*, vol. 10, no. 5, p. 5093, Oct., 2020.

[6] M. S. Islam, N. Mithulananthan, and D. Q. Hung, "A Day-ahead forecasting model for probabilistic EV charging loads at business premises," *IEEE Trans Sustain. Energy*, vol. 9, no. 2, pp. 741–753, Apr., 2018.

[7] R. Ghotge, Y. Snow, S. Farahani, Z. Lukszo, and A. van Wijk, "Optimized scheduling of EV charging in solar parking lots for local peak reduction under EV demand uncertainty," *Energies (Basel)*, vol. 13, no. 5, p. 1275, Mar., 2020.

[8] N. Kaewdornhan, C. Srithapon, R. Liemthong, and R. Chatthaworn, "Real-time multi-home energy management with EV charging scheduling using multi-agent deep reinforcement learning optimization," *Energies (Basel)*, vol. 16, no. 5, p. 2357, Mar., 2023.

[9] H. Wu, G. K. H. Pang, K. L. Choy, and H. Y. Lam, "An optimization model for electric vehicle battery charging at a

battery swapping station," *IEEE Trans. Veh. Technol.*, vol. 67, no. 2, pp. 881–895, Feb., 2018.

[10] X. Zhang, Y. Cao, L. Peng, N. Ahmad, and L. Xu, "Towards efficient battery swapping service operation under battery heterogeneity," *IEEE Trans. Veh. Technol.*, vol. 69, no. 6, pp. 6107–6118, Jun., 2020.

[11] Q. Lin, J. Wang, R. Xiong, W. Shen, and H. He, "Towards a smarter battery management system: A critical review on optimal charging methods of lithium ion batteries," *Energy*, vol. 183, pp. 220–234, Sep., 2019.

[12] M. Xu, R. Wang, P. Zhao, and X. Wang, "Fast charging optimization for lithium-ion batteries based on dynamic programming algorithm and electrochemical-thermal-capacity fade coupled model," *J. Power Sources*, vol. 438, p. 227015, Oct., 2019.

[13] Y. Li, K. Li, Y. Xie, J. Liu, C. Fu, and B. Liu, "Optimized charging of lithium-ion battery for electric vehicles: Adaptive multistage constant current–constant voltage charging strategy," *Renew. Energy*, vol. 146, pp. 2688–2699, Feb., 2020.

[14] Y.-H. Chiang, W.-Y. Sean, and J.-C. Ke, "Online estimation of internal resistance and open-circuit voltage of lithium-ion batteries in electric vehicles," *J. Power Sources*, vol. 196, no. 8, pp. 3921–3932, Apr., 2011.

[15] M. C. Argyrou, P. Christodoulides, C. C. Marouchos, and S. A. Kalogirou, "Hybrid battery-supercapacitor mathematical modeling for PV application using Matlab/Simulink," in *2018 53rd International Universities Power Engineering Conference (UPEC)*, IEEE, Sep., 2018.

[16] B. Yegnanarayana, *Artificial Neural Networks*. Delhi: PHI Learning Pvt. Ltd., 2009.

[17] J. L. Smith, "Advances in neural networks and potential for their application to steel metallurgy," *Materials Science and Technology*, vol. 36, no. 17, pp. 1805–1819, Nov., 2020.

[18] Z. Niu, Z. Yu, W. Tang, Q. Wu, and M. Reformat, "Wind power forecasting using attention-based gated recurrent unit network," *Energy*, vol. 196, p. 117081, Apr., 2020.

[19] Y. Zhang, J. Tang, Z. He, J. Tan, and C. Li, "A novel displacement prediction method using gated recurrent unit model with time series analysis in the Erdaohe landslide," *Natural Hazards*, vol. 105, no. 1, pp. 783–813, Jan., 2021.

[20] Y. Yu, X. Si, C. Hu, and J. Zhang, "A review of recurrent Neural Networks: LSTM cells and network architectures," *Neural Comput.*, vol. 31, no. 7, pp. 1235–1270, Jul., 2019.

[21] K. Smagulova and A. P. James, "A survey on LSTM memristive neural network architectures and applications," *Eur. Phys. J. Spec. Top.*, vol. 228, no. 10, pp. 2313–2324, Oct., 2019.

[22] A. A. Shalaby, M. F. Shaaban, M. Mokhtar, H. H. Zeineldin, and E. F. El-Saadany, "A dynamic optimal battery swapping mechanism for electric vehicles using an LSTM-based rolling horizon approach," *IEEE Transactions on Intelligent Transportation Systems*, vol. 23, no. 9, pp. 15218–15232, Sep., 2022.